# Halide Anion Recognition in Water by an Hexaprotonated Octaaza-Cryptand: A Molecular Dynamics Investigation

**Pierre Jost, Rachel Schurhammer, and Georges Wipff*[a]**

**Abstract:** Based on molecular dynamics simulations, we describe the $F^-$ versus $Cl^-$ complexation by an hexaprotonated cryptand $L^{6+}$ in aqueous solution, in order to elucidate their structures, solvation properties and the status of external halide counterions. In water, $F^-$ and $Cl^-$ simulated inclusive complexes adopt a structure somewhat different from the solid state structure of the $F^-$ complex: The anion binding involves two diammonium bridges only, and the accompanying counterions are dissociated from the $+5$ charged complex. A remarkable result is obtained for the dissociated $L^{6+}$,$3F^-$,$3Cl^-$ system, where spontaneous complexation of $F^-$ (the anion which forms the most stable complex with $L^{6+}$) takes place during the dynamics. The resulting complex is of facial type; this suggests that the equilibrium involves multiple binding modes and structures in aqueous solution. The question of $F^-/Cl^-$ binding selectivity is investigated by free energy perturbations simulations which nicely reproduce the spectacular preference for $F^-$ over $Cl^-$. Two different methodologies used for the treatment of electrostatics (standard versus Ewald calculations) yield similar conclusions.

**Keywords:** counterions · electrolytes · macrocycles · molecular dynamics · molecular recognition

## Introduction

Anion binding by macrocyclic hosts, early identified as a founding theme of supramolecular chemistry,[1–4] received relatively little attention, compared with cation binding.[5–8] The main reasons are presumably the limited choice of anion-binding sites (hydrogen bonds or Lewis acids), the larger size of the anions, and the role of solvent. In water, anions may be complexed by topologically connected macro(poly)cyclic ligands, whose ammonium-binding sites are positively charged, providing therefore, in addition to hydrogen bonding interactions, a strong electrostatic driving force for anion encapsulation. As far as modelling studies are concerned, the field of anion complexation is relatively unexplored. A recent review can be found in ref. [9]. Some molecular mechanics studies dealt with the gas phase behavior of these complexes,[10–13] while molecular dynamics (MD) simulations with explicit solvent tackled the question of competitive hydration and complexation processes.[10–12] The first paper on ion recognition in solution by a macrocyclic host concerned the $Cl^-/Br^-$ binding by a tetraprotonated SC24,$4H^{4+}$ tricyclic host.[13] For this system, the energy profile for $Cl^-$ anion inclusion has also been investigated by molecular mechanics in the gas phase,[14] as well as by MD in aqueous solution.[15, 16] Halide anion complexation by a neutral calixarene in organic solution has recently been reported.[17]

This paper deals with the halide anion complexation by an hexaprotonated bicyclic octaaza-cryptand (Figure 1), studied experimentally by Lehn et al.[18, 19] This ligand, referred to later as $L^{6+}$, forms in acidic aqueous solution, a complex with $F^-$ of high stability ($\log K = 10.55$, according to Lehn et al.[18] and 11.2 acording to Smith et al.[20]) and displays a spectacular $F^-/Cl^-$ selectivity ($> 10^8$). The inclusive nature of the $F^-$ complex, noted hereafter as $LF^{5+}$, is supported by NMR spectroscopy in solution, and by an X-ray structure,[18] where the six ammonium $N^+$ sites form a quasi trigonal prismatic arrangement with $F^- \cdots N^+$ distances ranging from 2.76 to

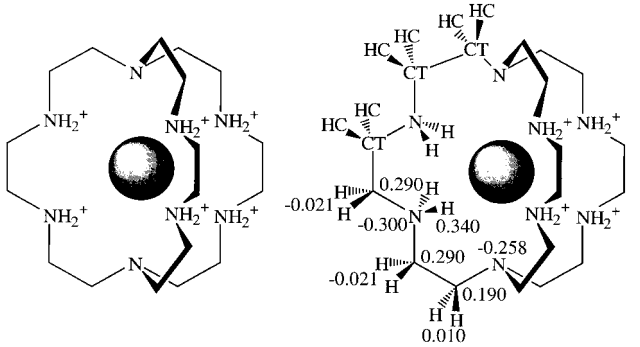


Figure 1. Schematic representation of the inclusion halide complex of $L^{6+}$ (left) with atomic charges and AMBER atom types used for the simulations (right).

[a] Prof. G. Wipff, P. Jost, R. Schurhammer
Laboratoire MSM, UMR 7551 CNRS, Institut de Chimie
4, rue B. Pascal, 67000 Strasbourg (France)
E-mail: wipff@chimie.u-strasbg.fr

Supporting information for this article is available on the WWW under http://www.wiley-vch.de/home/chemistry/ or from the author.

  0947-6539/00/0623-4257 $ 17.50+.50/0 

2.88 Å. These distances, typical for strong hydrogen bonds, are shorter than the two $F^- \cdots N$ distances with bridgehead nitrogens (3.28 and 3.37 Å). The three $^+NC-CN^+$ dihedrals are *gauche* (68, 74, and 74°, respectively), leading to a converging orientation of the ammonium binding sites. Due to the presence of the five other counterions ($2F^-$, $Cl^-$, and $2PF_6^-$), the symmetry of $LF^{5+}$ is slightly distorted from $D_3$.

Whether stuctures observed in a crystalline environment are representative of those present in aqueous solution is a recurrent question, which will be addressed by MD simulations. More specifically, we will first focus on the precise location of the complexed $F^-$, the conformation of the cage, and the location of the five accompanying counterions. Whether the structure with a given guest ($F^-$) is a good model for complexes involving larger guests (e.g. $Cl^-$) will be another matter of interest. Computer prediction of binding selectivities, in principle feasible through alchemical perturbations,[21] remains a challenge in computational chemistry, especially in the $LX^{5+}$ system studied herein, where, due to the high host–guest electrostatic forces, the selectivity likely results from small differences between numbers larger than those involved in ion complexation by neutral hosts. To our knowledge, the thermodynamic components of $\Delta G$ have not been determined for this system. However, based on the analysis of anion complexation by an analogous hexaprotonated hexacycle,[22, 23] where the entropic $T\Delta S$ component of $\Delta G$ is larger than the enthalpic $\Delta H$ component, it may be speculated that entropy effects also play a major role in the halide complexation and recognition by $L^{6+}$, a feature which is also quite challenging to account for computationally. Our MD simulations deal with the electroneutral $L^{6+}$,$3F^-$,$3Cl^-$ system, where the two $PF_6^-$ anions of the solid state structure have been replaced by $Cl^-$ anions.

First, we want to describe the $LF^{5+}$ and $LCl^{5+}$ inclusive complexes in water and compare their structures with the solid state analogue of $LF^{5+}$. We then consider the uncomplexed state, from simulations which start with all anions dissociated from $L^{6+}$. The main purpose is to examine the conformation of $L^{6+}$ uncomplexed, in relation with its possible preorganization. It will be shown that during the simulations, one anion ($F^-$) is spontaneously captured by the cryptand, which adopts a conformation somewhat different from the one in the solid state. The last section deals with the $F^-/Cl^-$ recognition, based on free energy perturbation calculations.

**Methods**: The molecular dynamics (MD) simulations were performed with the modified AMBER5 software[24] where the potential energy $U$ is given by:

$$U = \Sigma_{\text{bonds}} K_r (r - r_{eq})^2 + \Sigma_{\text{angles}} K_\theta (\theta - \theta_{eq})^2 + \Sigma_{\text{dihedrals}} \Sigma_n V_n (1 + \cos n\phi) + \Sigma_{i<j} [q_i q_j / R_{ij} - 2\varepsilon_{ij} (R_{ij}^*/R_{ij})^6 + \varepsilon_{ij} (R_{ij}^*/R_{ij})^{12}]$$

The electrostatic and van der Waals interactions between atoms separated by at least three bonds are described within a pairwise additive scheme by a 1-6-12 potential. Parameters for the solutes were taken from the AMBER force field[25] and from previous studies.[10] Atom types and charges are summarized in Figure 1. The atomic charges on $L^{6+}$ were fitted from ESP calculations.[10] They were used without a special scaling factor for 1–4 interactions. Noteworthy is the $N^{-0.30}$ $H^{+0.34}$ polarity of the ammonium bonds, similar to the values of Papoyan et al. ($N^{-0.30}$ $H^{0.45}$).[12] The Lennard-Jones parameters of the $F^-$ and $Cl^-$ anions ($R^*_F = 1.850$; $R^*_{Cl} = 2.495$ Å; $\varepsilon_F = 0.200$; $\varepsilon_{Cl} = 0.107$ kcal mol$^{-1}$) have been fitted to reproduce their relative free energies of hydration.[26] The water molecules were represented by the TIP3P model.[27]

Long range electrostatic forces are particularly important for charged systems and may critically determine their dynamic behavior.[28] This is why two types of simulation conditions have been compared. The first one (noted 15-std) uses a standard treatment of electrostatics with a 11/15 Å twin cutoff distance. The second one (noted 11 + PME) uses the PME (particle mesh Ewald) treatment of electrostatics, as implemented in AMBER5, in conjunction with a residue based cutoff of 11 Å. Each anion and $L^{6+}$ were considered as single residues. Discontinuties in the potential energy may translate into spurious values and fluctuations of temperatures. Thus, after several tests (Supporting Information, Table S1), we decided to separately couple the solvent and solute parts of the system to a thermal bath at 300 K, based on the Berendsen algorithm[29] with a relaxation time $\tau_T$ of 0.1 ps. In all cases, the average temperature $\langle T \rangle$ was $300 \pm 3$ K for water as for the whole system, but displayed significant variations and fluctuations for the anions at a temperature of about $320 \pm 90$ K in the 15-std calculations and $290 \pm 90$ K with the $11 \pm$ PME. We also tested the effect of a reaction field correction[30] with a 11/15 Å twin cutoff, and found the temperatures of the ligand and anions are close to those obtained with the 11 + PME conditions. Thus, the 15-std and 11 + PME simulations correspond to models where the anions are either "cold" and "warm". In all simulations, the pairlists for non-bonded interactions were updated every 10 fs.

The solute was immersed in a "cubic" box of about 45 Å length, containing about 2600 water molecules (see Figure 2 and Table 1). This corresponds to a ligand concentration of

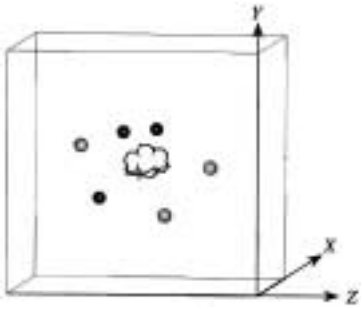


Figure 2. Simulation box with the starting structure of the $L^{6+}$, $3F^-$, $3Cl^-$ system.

$1.9 \times 10^{-2}$ mol L$^{-1}$, about ten times more concentrated than in the complexation experiments reported by Lehn et al.[18] or Smith et al.[20]. After 4000 steps of energy minimization with conjugate gradients, 20 ps of MD were performed keeping the solute rigid (BELLY option of AMBER),[25] allowing for water relaxation. Then, MD was run without constraints for timescales ranging from 0.4 to 1.3 ns (Table 1). The simulated



0947-6539/00/0623-4258 $ 17.50+.50/0 *Chem. Eur. J.* **2000**, *6*, No. 23

Table 1. Simulation conditions of the $L^{6+}$, $3F^-$, $3Cl^-$ systems.

| System | Cutoff [Å] | Time [ns] | Box size ($x \times y \times z$) [Å$^3$] | $N_{water}$ |
|---|---|---|---|---|
| $LF^{5+}$, $2F^-$, $3Cl^-$ | 11 + PME | 1.15 | 47.5 × 44.9 × 42.0 | 2647 |
| | 15-std | 0.9 | 47.5 × 44.9 × 42.0 | 2647 |
| $LCl^{5+}$, $2F^-$, $3Cl^-$ | 11 + PME | 1.0 | 47.5 × 44.9 × 42.0 | 2647 |
| | 15-std | 0.4 | 47.5 × 44.9 × 42.0 | 2647 |
| $L^{6+}$, $3F^-$, $3Cl^-$ | 11 + PME | 1.3 | 44.2 × 44.2 × 44.2 | 2501 |
| | 15-std | 0.6 | 44.2 × 44.2 × 44.2 | 2501 |

solvent systems are described in Table 1. All C–H, N–H, O–H, H···H bonds were constrained with SHAKE, using a step of 1 fs.

**Binding selectivity and free energy calculations**: The difference in Gibbs free energies ($\Delta G$) between systems A ($F^-$) and B ($Cl^-$) were calculated with the free energy perturbation (FEP) method in the standard simulations (no Ewald) while the thermodynamics integration (TI) method was used for calculations using PME. Indeed, PME is not implemented in AMBER5 for FEP calculations. Both FEP and TI methods were combined with a windowing technique, based on the following equations:

TI method:

$$\Delta G = \int_{\lambda=0}^{1} \left\langle \frac{\partial U}{\partial \lambda} \right\rangle_{\lambda} \mathrm{d}\lambda$$

FEP method:

$$\Delta G = \Sigma \Delta G_{\lambda} \text{ and } \Delta G_{\lambda} = RT \log \left\langle \exp \frac{(U_{\lambda} - U_{\lambda+\Delta\lambda})}{RT} \right\rangle_{\lambda}$$

At each window (i.e., at each $\lambda$), 2 ps of equilibration and 3 ps of data collection were performed. The mutations were achieved in 21 or 51 equally spaced windows.

The variations of the potential energy $U_{\lambda}$ were calculated using a linear combination of the $\varepsilon_{ij}$ and $R_{ij}$* parameters of the initial state ($\lambda = 1$) and the final state ($\lambda = 0$):

$$\varepsilon(\lambda) = \lambda\,\varepsilon(1) + (1-\lambda)\,\varepsilon(0) \text{ and } R^*(\lambda) = \lambda\,R^*(1) + (1-\lambda)\,R^*(0)$$

For FEP mutations, the $\Delta G$ values were accumulated "forward" and "backward". We report the average values.

**Analysis of results**: Average structural features and energy components were analyzed from the trajectories saved every picosecond using the MDS and DRAW software.[31] The interaction energies between the different groups and the solvent were recalculated from the trajectories. The average hydration characteristics were obtained by radial distribution functions "RDFs" of water around selected centers. The "center of the cage" (CM) was calculated at each step as the center of mass of its non-hydrogen atoms.

## Results

The main structural and energy features simulated complexes are summarized in Table 2. Figure 4, Figure 6 and Figure 7 display selected structures along the dynamics, with the time evolution of the shortest $L^{6+}\cdots X^-$ distances, obtained with the 11 + PME methodology. The corresponding 15-std results are displayed in Figures S1 to S3 in the Supporting Information. Although most simulations have been performed with both 15-std and 11 + PME methodologies, with mostly focus on the 11 + PME results, obtained from longer simulations ($\geqslant$ 1 ns).

**The $LF^{5+}$ and $LCl^{5+}$ "inclusive" complexes in water and the structures, hydration and status of accompanying counterions**: All simulations of the $LF^{5+}$ and $LCl^{5+}$ inclusive complexes started with the solid state structure of the inclusive $F^-$ complex, adding either $2F^-$ or $3Cl^-$ neutralizing the counterions (Figure 3). One anion was initially at the center of the cryptand's cavity, the others being at 3.7, 4.1, 4.5, 8.4 and 7.4 Å from the center of $L^{6+}$ as in the solid state structure of the $LF^{5+}$ complex.[18]

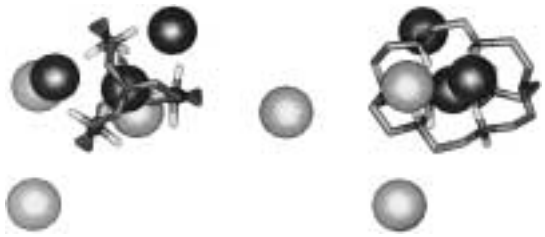

Figure 3. The $LF^{5+}$ inclusive complex. Solid state structure (orthogonal views) where the two external $PF_6^-$ anions have been replaced by $Cl^-$ anions in the simulations (0 ps). From ref. [18].

We first discuss $LF^{5+}$. Interestingly, during the first 200 ps, an anion exchange is observed, where the inclusive $F^-$ moves to facial position of the ligand, and is replaced by another facial $F^-$ anion at the center of $L^{6+}$ (Figure 4). An intermediate state is observed, where each of the three $F^-$ anions sits on a face of $L^{6+}$, at about 2.5 Å from the cavity which is empty (Figure 4). Thus, during the first 0.5 ns, the three fluoride anions are in contact with, or complexed by $L^{6+}$, while the three chlorides slowly dissociate beyond the cutoff distance. Further dissociation of two uncomplexed $F^-$ anions takes place at a later stage, at 0.5 and 0.7 ns, respectively. Analysis of the trajectories reveals that their dissocation requires the assistance of at least three hydrogen bonded water molecules. The final state of $LF^{5+}$ corresponds to fully dissociated counterions and to a complex somewhat different from the one in the solid state, where $F^-$ is more "facial", at $0.8 \pm 0.1$ Å from the center of $L^{6+}$, bound by two bridges only of the cryptand. The corresponding $^+NC–CN^+$ dihedrals are of *gauche* type ($86 \pm 14^\circ$), while the third diammonium moiety, not involved in the anion binding, is more open ($134 \pm 14^\circ$) and points its $NH_2^+$ protons outwards. The complex is thus of about $C_{2v}$ symmetry. There are four $F^-\cdots N^+$ distances of 2.95 to 3.00 Å, about 0.3 Å longer than in the crystal, and two $F^-\cdots N^+$ distances at $4.7 \pm 0.2$ Å. The size of the cage, defined by the $N_{bridgehead}\cdots N_{bridgehead}$ distances is $6.4 \pm 0.2$ Å, i.e. about 0.2 Å shorter than in the crystal. The plot of the $NH^+\cdots F^-$ distances during the last 0.2 ns of the simulation (Figure 4) shows that $F^-$ is hydrogen bonded to four $NH_2^+$ groups, each of them with one proton at 2.1 Å and another proton at 3.7 Å

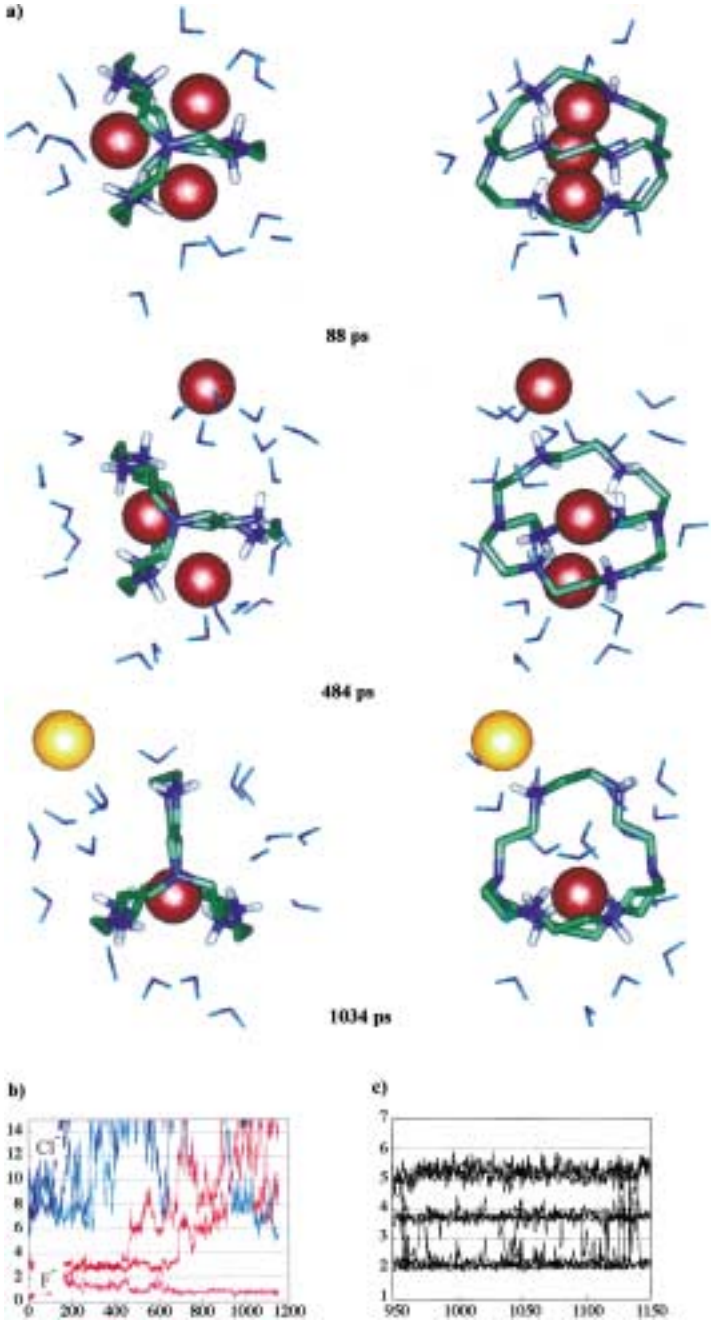


Figure 4. a) The $LF^{5+}$, $2F^-$, $3Cl^-$ complex simulated in water (11 + PME calculations). Snapshots after 88, 484, and 1034 ps with selected first shell water molecules (orthogonal views). b) Time evolution of the distances (shorter than 15 Å) between the anions and the cavity center of $L^{6+}$. c) Distances between the complexed anion and the 12 NH protons during the last 200 ps.

from $F^-$, while the four $NH^+$ protons of the "unbound bridge" are too far (5.2 Å) to bind $F^-$.

Concerning the hydration of $LF^{5+}$, the radial distribution functions (Figure 5) show that the complexed anion is fully shielded from water, and that the orientation of water molecules is mostly determined by the positive charge of $L^{6+}$: the first $F^- \cdots O_{water}$ and $F^- \cdots H_{water}$ peaks are at about 3.9 and 4.8 Å, respectively. The four $NH^+$ protons pointing to $F^-$ are not hydrated, while all others are hydrogen bonded by about 1.7 water molecules (at a $NH^+ \cdots O_w$ distance of 1.82 Å).

The structure obtained with the 15-std conditions is similar as far as the inclusive binding of $F^-$ is concerned. During 0.80 ns, one external $F^-$ anion remained facially bound to the ligand, at about 3 Å from the center of $LF^{5+}$ (Figure S1), but finally dissociated to bulk water like the other anions.

The chloride complex $LCl^{5+}$, simulated with the 11 + PME method, showed a behavior similar to $LF^{5+}$ (Figure 6). The complexed anion remained more or less inside the cavity of the ligand while the three other $Cl^-$ and two $F^-$ counterions also dissociated from $L^{6+}$. Interestingly, the complexed $Cl^-$ was at the center of the cavity of the ligand for the first 0.6 ns, but then moved to a facial position, at about 1.0 Å from the center. Finally, the $^+NC–CN^+$ dihedrals are more open (124°, 121°, and 127 ± 15°) than in the fluoride complex, in relation with the larger size of the guest. The strain induced by $Cl^-$ can be seen in the smaller difference between $Cl^- \cdots N_{bridgehead}$ (3.4 Å) and $Cl^- \cdots N^+$ distances (from 3.3 to 3.5 Å). Again, $Cl^-$ is facially coordinated by four $NH^+$ protons (at about 2.9 Å, their geminal protons being at 4.3 Å) of two diammonium bridges. The $NH^+$ protons of the third bridge are more remote (5.4 Å). According to the analysis of the RDF values, the complexed $Cl^-$ is also fully shielded from water. The first peak is observed at about 3.9 Å for the $F^- \cdots O_{water}$ RDF, which indicates that water dipoles are oriented by the positive charge of the ligand; this leads therefore to repulsive interactions with the anionic guest.

The energy component analysis on the $LF^{5+}$ and $LCl^{5+}$ inclusive complexes (Table 2) indicates that, intrinsically, the former is about 20 kcal mol$^{-1}$ more stable, mostly due to the enhanced ligand–anion interactions ($\Delta E = 70$ kcal mol$^{-1}$), while the ligand within the complex is less stable ($\Delta E =$ 50 kcal mol$^{-1}$; Table 2). Both $LF^{5+}$ and $LCl^{5+}$ species display similar interactions with water. Interestingly, the anion–water interactions are repulsive in both systems (about 177 with $F^-$ and 165 ± 12 kcal mol$^{-1}$ with $Cl^-$), which indicates that solvation of the complex is dominated by its +5 charge and is antagonist to the anion hydration. Upon complexation, the anion hydration becomes unfavorable and this energy penalty contributes to the overall binding selectivity (vide infra). This may be a specific feature of ion binding by positively charged ammonium binding sites, compared with the anion binding by neutral hosts, which likely translates into marked entropy changes due to solvent reorganization.

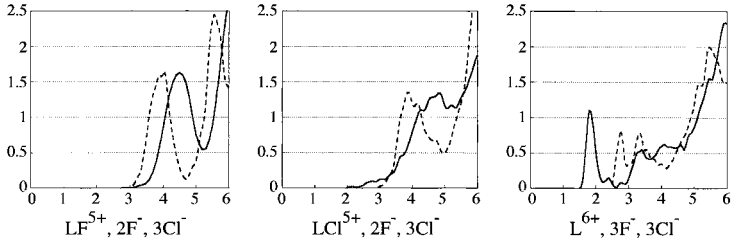


Figure 5. The $LF^{5+}$ and $LCl^{5+}$ complexes and the uncomplexed ligand in water. $H_w$ (full line) and $O_w$ (dotted line) RDF values around the complexed anion and around the center of $L^{6+}$ (11-PME calculations).



0947-6539/00/0623-4260 $ 17.50+.50/0 Chem. Eur. J. 2000, 6, No. 23

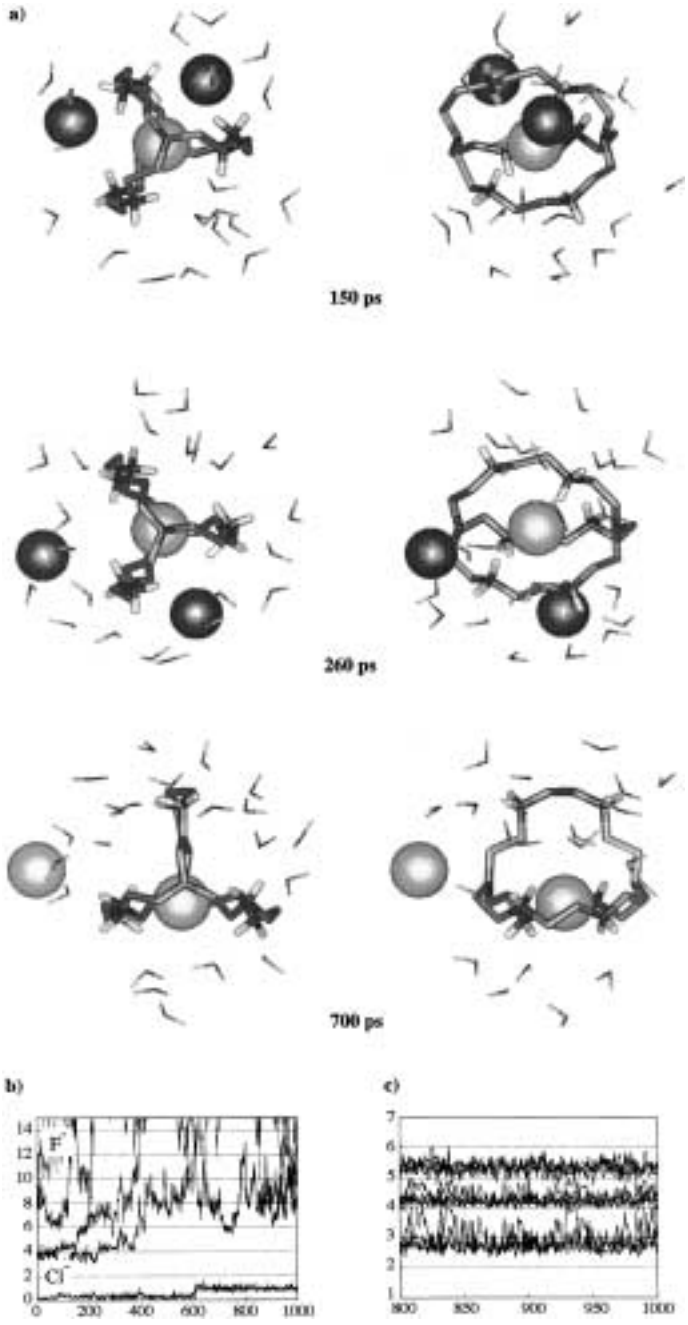


Figure 6. a) The $LCl^{5+}$, $2F^-$, $3Cl^-$ complex simulated in water (11 + PME calculations). Snapshots after 150, 260, and 700 ps with selected first shell water molecules (orthogonal views). b, c) See Figure 4. A color version of this Figure is available as Suppporting Information (Figure S4).

Again, comparison of 11 + PME and 15-std results (Figure S2 and Table 2) leads to similar structural and energy features.

**Simulation of $L^{6+}$ (uncomplexed), $3F^-$, $3\,Cl^-$ leads to spontaneous capture and recognition of $F^-$ by the cryptand**: The uncomplexed $L^{6+}$ cryptand was simulaled in the presence of the six neutralizing counterions, initally placed at 9 to 14 Å from the center of the cavity, with 11 + PME and 15-std methodologies. In both simulations, due to its internal electrostatic strain, the cryptand rapidly underwent a swelling distortion and conformational changes, while all six $NH_2^+$ groups moved to "diverging" orientations and the $^+NC{-}CN^+$ dihedrals became nearly *trans*. At the beginning of the dynamics, all anions diffused in water, some of them remaining far beyond the cutoff distances, while others moved inside the cutoff distance of $L^{6+}$.

In the 11 + PME simulation, two remarkable events took place. The first one began at 0.38 ns, where one $Cl^-$ anion was attracted by $L^{6+}$, at about 4.2 Å from the center of the ligand. As shown in Figure 7, this anion was loosely coordinated on one face of the cryptand, and remained there for about 50 ps. Despite the high electrostatic attraction with $L^{6+}$, it then fully dissociated to the bulk solution at about 0.8 ns. This dissociation was concomitant with the approach of one $F^-$ anion from the bulk solution, to a short contact distance with the ligand. From 0.8 to 1.3 ns, this anion was progressively captured by $L^{6+}$, to form a stable inclusive complex (Figure 7). This simulation thus reveals the *spontaneous* selection of $F^-$ by the ligand in the presence of $Cl^-$ competiting species. The final structure differs, however, from the structures of $LF^{5+}$ described above: One $^+NC\text{-}CN^+$ dihedral is *trans* ($180 \pm 10^\circ$), one is $117 \pm 8^\circ$ and the third one, more involved in the fluoride binding, is nearly *gauche* ($-80 \pm 8^\circ$). Finally, $F^-$ is hydrogen bonded to two $NH^+$ protons at 2.10 Å, the two geminal hydrogens being at 3.7 Å and the remaining eight $NH^+$ being at 4.5 to 5.0 Å. The $F^-$ anion is somewhat less shielded from water than in the structure obtained at the end of the simulation of the "inclusive complex". According to the $F^- \cdots H_{water}$ radial distribution function, it is hydrogen-bonded to 0.4 water molecules.

Performing the simulation with the 15-std conditions (no Ewald) similarly led to the spontaneaous complexation of one $F^-$ anion, but earlier (at about 0.4 ns) than with the 11 + PME calculations (Figure S3). Again, excursions to "precomplexation processes" of both types of anions could be recognized, but only $F^-$ was captured. The final conformation of the complex was again somewhat different. Two $^+NC{-}CN^+$ dihedrals were *trans* ($180 \pm 7^\circ$) and the other was *gauche* $80 \pm 10^\circ$. As complexation seemed to rigidify the ligand, the simulations were stopped 300 ps after the complex was formed, while retaining a constant conformation and anion binding mode. Here, $F^-$ binds to two $NH^+$ of one bridge only (at 2.1 Å). The two geminal ones are at 3.6 Å, and the eight remaining $NH^+$ at are 4.5 to 5.2 Å.

The energy component analysis (Table 2) shows that this fluoride complex displays weaker anion–host interactions than the $LF^{5+}$ inclusive complex described above ($\Delta E = 38$ kcal mol$^{-1}$), but is better hydrated (by about 40 kcal mol$^{-1}$).

**The $Cl^-$ versus $F^-$ binding selectivity from free energy perturbation calculations**: The $Cl^-$ versus $F^-$ binding selectivity by the cryptand, defined experimentally as $\Delta\Delta G_c = \Delta G_1 - \Delta G_2$, was obtained computationally by the "alchemical route" as $\Delta\Delta G_c = \Delta G_3 - \Delta G_4$, where $\Delta G_3$ corresponds to the difference in hydration free energies of $F^-$ versus $Cl^-$, and $\Delta G_4$ corresponds to the difference in free energies between $LF^{5+}$ and $LCl^{5+}$ complexes, in the presence of the neutralizing counterions $X^-$ in solution.

Table 2. Average structural features and energy components of the $L^{6+}$, $3F^-$, $3Cl^-$ systems simulated in water. 15-std and 11 + PME results. Average are over the last 200 ps.

| | X-ray | $LF^{5+}$, $2F^-$, $3Cl^-$ | | $LCl^{5+}$, $2F^-$, $3Cl^-$ | | $L^{6+}$, $3F^-$, $3Cl^-$ | |
|---|---|---|---|---|---|---|---|
| | | 11 + PME | 15-std | 11 + PME | 15-std | 11 + PME | 15-std |
| | | | | Geometry parameters[a] | | | |
| $X^- - CM$[b] | 0.064 | 0.76 ± 0.13 | 0.80 ± 0.24 | 0.96 ± 0.15 | 0.29 ± 0.12 | 0.71 ± 0.14 | 0.65 ± 0.11 |
| $X^- - N_2$ | 2.762 | 2.97 ± 0.10 | 2.93 ± 0.12 | 3.36 ± 0.14 | 3.51 ± 0.22 | 4.00 ± 0.15 | 3.90 ± 0.10 |
| $X^- - N_3$ | 2.875 | 2.95 ± 0.10 | 2.95 ± 0.12 | 3.49 ± 0.25 | 3.49 ± 0.23 | 3.92 ± 0.15 | 3.85 ± 0.10 |
| $X^- - N_5$ | 2.783 | 3.00 ± 0.10 | 2.93 ± 0.11 | 3.34 ± 0.10 | 3.57 ± 0.26 | 4.51 ± 0.16 | 3.36 ± 0.10 |
| $X^- - N_6$ | 2.821 | 2.95 ± 0.20 | 2.97 ± 0.10 | 3.36 ± 0.15 | 3.60 ± 0.25 | 4.46 ± 0.14 | 3.29 ± 0.11 |
| $X^- - N_7$ | 2.841 | 4.66 ± 0.20 | 4.62 ± 0.27 | 4.79 ± 0.16 | 3.40 ± 0.29 | 2.98 ± 0.10 | 4.00 ± 0.11 |
| $X^- - N_8$ | 2.856 | 4.67 ± 0.22 | 4.60 ± 0.24 | 4.79 ± 0.15 | 3.52 ± 0.23 | 2.95 ± 0.10 | 4.14 ± 0.10 |
| $N_1 - N_4$ | 6.644 | 6.39 ± 0.22 | 6.44 ± 0.20 | 6.50 ± 0.16 | 6.81 ± 0.15 | 6.2 ± 0.2 | 6.20 ± 0.16 |
| $\langle X^-(out) - CM\rangle$[c] | 5.612 | 15.6 ± 0.9 | 11.5 ± 0.8 | 17 ± 3 | 11.6 ± 0.7 | 19 ± 3 | 13 ± 1 |
| $^+N_2C - CN_3^+$ | 74 | 86 ± 12 | 90 ± 15 | 124 ± 21 | 135 ± 20 | 180 ± 8 | − 118 ± 9 |
| $^+N_5C - CN_6^+$ | 68 | 87 ± 12 | 82 ± 12 | 121 ± 21 | 137 ± 24 | 117 ± 8 | 81 ± 8 |
| $^+N_7C - CN_8^+$ | 73 | 134 ± 16 | 120 ± 10 | 127 ± 10 | 130 ± 30 | − 81 ± 8 | − 179 ± 7 |
| | | | | Energy components[d] | | | |
| $E$(L) | | 1180 ± 18 | 1175 ± 11 | 1130 ± 8 | 1150 ± 76 | 1120 ± 7 | 1125 ± 7 |
| $E$(L/X)[e] | | − 561 ± 8 | − 565 ± 9 | − 490 ± 7 | − 511 ± 10 | − 523 ± 15 | − 525 ± 4 |
| $E$ (X/water) | | 177 ± 13 | 213 ± 18 | 165 ± 12 | 195 ± 12 | 172 ± 12 | 211 ± 10 |
| $E$ (L/water) | | − 1180 ± 50 | − 1580 ± 80 | − 1150 ± 50 | − 1380 ± 70 | − 1220 ± 80 | − 1540 ± 80 |

[a] Distances in Å and dihedral angles in degrees. [b] Distance between the complexed anion $X^-$ and the center of mass CM of $L^{6+}$. [c] Average distance between the five uncomplexed anions and the center of $L^{6+}$. [d] In kcal mol$^{-1}$. [e] Interaction energy between $L^{6+}$ and the complexed anion X.

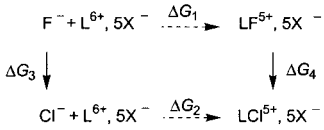


FEP simulations were performed with the 11 + PME methodology, but the 15-std conditions was tested in some cases. The results are reported in Table 3. The $\Delta G_3$ energies were first calculated on the isolated anion ($Cl^-/F^-$). The corresponding values (27.4 with 15-std and 28.2 kcal mol$^{-1}$ with 11 + PME), are similar and close to the experimental value of 29.8 kcal mol$^{-1}$;[32] this shows that they are little influenced by the treatment of "long range electrostatics". A second set of mutations was performed on one external $F^-$ anion of the $LF^{5+}$, $2F^-$, $3Cl^-$ system, which was mutated to $Cl^-$. The $\Delta G_3$ values were within 0.1 kcal mol$^{-1}$ identical to those obtained with the isolated anion, with the 11 + PME and 15-std methods.

The $\Delta G_4$ energies were obtained from four independent runs where the complexed $F^-$ anion was mutated to $Cl^-$, or vice versa. In all cases, the anion remained encapsulated, bound by two diammonium bridges of the cryptand only. We first perfomed two $LCl^{5+} \rightarrow LF^{5+}$ mutations starting from the same state (1 ns of 11 + PME dynamics on the $LCl^{5+}$ complex) and using identical sampling (21 windows). The first one used the 15-std and second one used 11 + PME conditions. They led to somewhat different $\Delta G_4$ values (− 47.9 and − 41.7 kcal mol$^{-1}$, respectively). Repeating the 11 + PME mutations with enhanced sampling (51 windows) led to similar results as with 21 windows (− 42.6 kcal mol$^{-1}$), which indicates that the sampling was sufficient. In order to check for possible hysteresis, we also mutated $LF^{5+} \rightarrow LCl^{5+}$ with the 11 + PME method, starting after 1.15 ns of MD. The $\Delta G_4$ energy change was 41.4 kcal mol$^{-1}$, indicating that there should be no problem of hysteresis. Thus, all 11 + PME results, a priori more satisfactory than the 15-std ones, are quite close to each other.

Table 3. Results of free energy perturbation simulations in water ($\Delta G$ in kcal mol$^{-1}$).

| Mutation | Simulations conditions | Windows | $\Delta G_3$ | $\Delta G_4$ |
|---|---|---|---|---|
| $F^- \rightarrow Cl^-$ | 15-std | 21 | 27.4 | |
| $F^- \rightarrow Cl^-$ | 11 + PME | 21 | 28.2 | |
| $F^- \rightarrow Cl^-$ | 11 + PME | 51 | | 41.4 |
| $Cl^- \rightarrow F^-$ | 15-std | 21 | | − 47.9 |
| $Cl^- \rightarrow F^-$ | 15 + PME | 21 | | − 41.7 |
| $Cl^- \rightarrow F^-$ | 11 + PME | 51 | | − 42.6 |

Combining the $\Delta G_3$ (28.2 kcal mol$^{-1}$) and average $\Delta G_4$ (42.0 kcal mol$^{-1}$) values obtained consistently with 11 + PME leads to a selectivity $\Delta\Delta G_c$ of 13.8 kcal mol$^{-1}$. As noted above, two somewhat different stability constants have been reported for the fluoride complex ($\log K(F^-) = 10.55$[18] and 11.2[20]; likely in relation to the difference in supporting electrolytes (0.1M $(Me_4N)TsO$ and 0.1M $KNO_3$, respectively). Similarly, $\log K(Cl^-)$ for the hexaprotonated chloride complex can be estimated to be $< 1.52$[20] and $< 2$[18]. Considering the average experimental values leads to $\log K(F^-) = 10.9$ and $\log K(Cl^-) = 1.75$, which translates to the $\Delta\Delta G_c$ energy difference of 12.3 ± 0.7 kcal mol$^{-1}$. Our calculated selectivity is in good agreement with this result.

## Discussion and Conclusion

We report a MD study on the aqueous solution behavior of an hexaprotonated cryptand and its halide complexes. A first question, which stimulated our study, deals with the role of external counterions and of hydration on the precise structure of the $LF^{5+}$ complex, as in the crystalline form, several counterions make short contacts with the positively charged $LF^{5+}$ species. During the dynamics the external anions fully dissociate to the bulk solution, leaving $LF^{5+}$ fully hydrated. This feature is observed with two different treatments of the electrostatics, and for $F^-$ and $Cl^-$ anions as guests. This may a



0947-6539/00/0623-4262 $ 17.50+.50/0 Chem. Eur. J. 2000, 6, No. 23

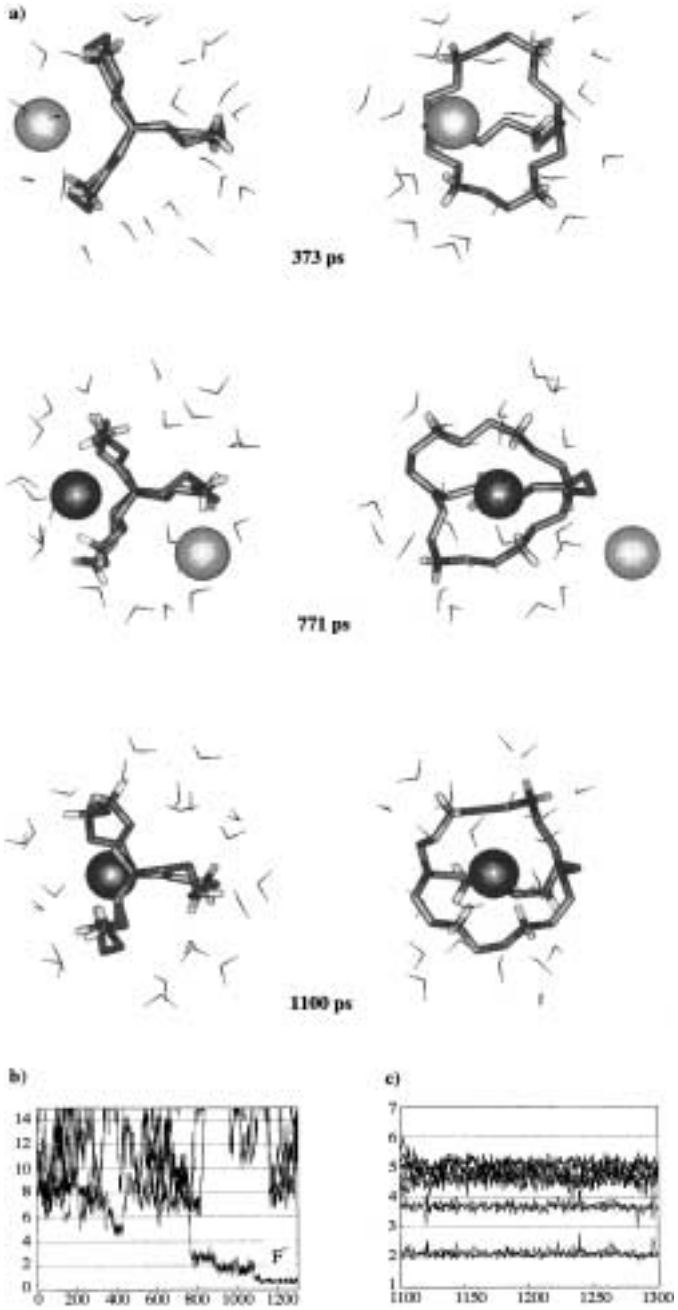


Figure 7. a) The uncomplexed $L^{6+}$, $3F^-$, $3Cl^-$ system simulated in water (11 + PME calculations). Snapshot at 373, 771 and 1100 ps with selected first shell water molecules (orthogonal views). b, c) See Figure 4. A color version of this Figure is available as Suppporting Information (Figure S5).

posteriori justify the neglect of external counterions in the previous studies of anion complexes of highly charged ligands such as $SC24,4H^{4+}$[13, 16] or $[24]\text{-}N_6O_2^{6+}$[12]. As our simulated systems are more concentrated than those studied experimentally by Lehn et al.[18] or Smith et al.,[20] ion dissociation should be still more effective in these experimental conditions. In the solid state, the two external facially coordinated $F^-$ anions likely lock the cryptand in a nearly threefold symmetrical arrangement, where a $F^-$ guest is encapsulated. In aqueous solution, dissociation of external anions is followed by a conformational transition of the fluoride or chloride complexes, where the anion is held by two diammonium moieties of the ligand only. The third diammonium bridge adopts a diverging orientation, due to main effects: This somewhat reduces the internal electrostatic strain of the ligand, and enhances its hydration. We also notice that water interacts repulsively with the complexed anion. When the latter moves from the fully encapsulated position (as in the solid state structure) to a less symmetrical form, it also becomes somewhat accessible to water. There are thus several arguments in favor of a less symmetrical structure in water, compared with the solid state. In principle, if the simulations were long enough, the role of the three diammonium briges should intervert, leading to an average structure of threefold symmetry. This does not occur on the nanosecond timescale, however, likely because the energy barrier for anion exchanging from one face to the other may be too high.

The relaxation times of highly charged systems may be larger than in neutral ligands and simulations have to be carried out long enough. Each simulation with Ewald was run for at least one nanosecond and such a duration was essential to observe the *spontaneous* capture of one of the anions. This is, to our knowledge, the first report of spontaneous ion binding by a polycyclic ligand. Noteworthy is also the *anion* selection, as pre-complexation of a chloride anion was observed during the simulation, but turned out to be non-productive.

Concerning the simulated anion binding mode, we notice that it is achieved locally through "linear" charge-dipole $X^-\cdots H\text{-}N$ interactions, as in the solid state structure, rather than by bridging interaction involving the two $NH_2^+$ protons. This leaves the second proton free to hydrogen bond to nearby water molecules. Somewhat different conformations were observed for the structures obtained from the inclusive complex, or from the spontaneaous complexation. As they did not interchange at the simulated timescales, it is not possible to conclude on which one is the most stable. It may also be suggested that anion complexation involves somewhat different binding modes and conformations in solution, different from the solid state analogue. Additional ions from the supporting electrolytes (which are about 100 times more concentrated than the cryptand) may also modulate these structures.

Our free energy calculations successfully account for the high $F^-/Cl^-$ binding selectivity, which mostly stems from the higher interactions with the cryptand ($\Delta G_4$ energy component). Although enthalpy and entropy components cannot be assessed from our simulations, we notice that $\Delta G_4$ is dominated by the larger anion–host interactions which are partly compensated, however, by the somewhat higher strain of the ligand and more repulsive hydration in the complexed $F^-$ anion.

The success of the calculations is quite encouraging and illustrates the utility of molecular dynamics simulations with explicit solvation and using well known force fields, to gain microscopic insights into host–guest complexes and their environment.

**Note added in proof**: We recently repeated two MD simulations to explore the role of internal electrostatic strain on the structures in solution. For this purpose, the 1–4

electrostatic interactions of the ligand were divided by 2.0 (SCEE = 2.0), while the above-reported results correspond to SCEE = 1.0. We used the PME method with a 12 Å cut-off. The first simulation started with the solid-state structure of the complex and was run for 0.7 ns. The $Cl^-$ anions moved to the bulk, while the three $F^-$ anions remained facially coordinated to $L^{6+}$, instead of dissociating when SCEE = 1. The second simulation of 0.4 ns started with the fully dissociated counterions. One $F^-$ was captured (at 0.22 ns), leading to a structure similar to the one observed with SCEE = 1. Thus, scaling down the internal electrostatic strain by 2.0 confirms the conclusions obtained with SCEE = 1.

## Acknowledgement

The authors are grateful to the Université Louis Pasteur (Strasbourg) and IDRIS CNRS for computer resources. R. S. thanks the French Ministry of Research for a grant.

[1] B. Dietrich, J. M. Lehn, J. P. Sauvage, J. Blanzat, *Tetrahedron* **1973**, *29*, 1629 – 1645.
[2] J.-M. Lehn, *Acc. Chem. Res.* **1978**, *11*, 49 – 57.
[3] J.-M. Lehn, *Pure Appl. Chem.* **1978**, *50*, 871 – 892.
[4] J.-M. Lehn, *Angew. Chem.* **1988**, *100*, 91 – 116; *Angew. Chem. Int. Ed. Engl.* **1988**, *27*, 89 – 112; B. Dietrich, *Pure Appl. Chem.* **1993**, *65*, 1457 – 1464.
[5] J.-M. Lehn, *Supramolecular Chemistry. Concepts and Perspectives*, VCH, Weinheim, **1995**.
[6] A. Bianchi, K. Bowman-James, E. Garcia-Espana *Supramolecular Chemistry of Anions*, Wiley-VCH, New York, **1997**.
[7] F. P. Schmidtchen, M. Berger, *Chem. Rev.* **1997**, *97*, 1609 – 1646.
[8] R. M. Izatt, K. Pawlak, J. S. Bradshaw, *Chem. Rev.* **1991**, *91*, 1721 – 2085.
[9] J. Wiorkiewicz-Kuczera, K. Bowman-James in *Supramolecular Chemistry of Anions* (Eds.: A. Bianchi, K. Bowman-James, E. Gracia-Espana), Wiley-VCH, New York, **1997**, pp. 335 – 354.
[10] S. Boudon, A. Decian, J. Fischer, M. W. Hosseini, J. M. Lehn, G. Wipff, *J. Coord. Chem.* **1991**, *23*, 113 – 135.
[11] S. Boudon, G. Wipff, *J. Chim. Phys.* **1991**, *88*, 2443 – 2449.
[12] G. Papoyan, K.-J. Gu, J. Wiorkiewics-Kuczera, K. Kuczera, K. Bowman-James, *J. Am. Chem. Soc.* **1996**, *118*, 1354 – 1364.
[13] T. P. Lybrand, J. A. McCammon, G. Wipff, *Proc. Natl. Acad. Sci. USA* **1986**, *83*, 833 – 835.
[14] G. Wipff, J. M. Wurtz, *New J. Chem.* **1989**, *13*, 807 – 820.
[15] B. Owenson, R. D. MacElroy, A. Pohorille, *THEOCHEM* **1988**, *179*, 467 – 484.
[16] B. Owenson, R. D. MacElroy, A. Pohorille, *J. Am. Chem. Soc.* **1988**, *110*, 6992 – 7000.
[17] N. A. McDonald, W. P. van Hoorn, E. M. Duffy, W. L. Jorgensen in *Supramolecular Science*: *Where It Is and Where It Is Going* (Eds.: R. Ungaro, E. Dalcanale), Kluwer, Dordrecht, **1999**, pp. 147 – 156; N. A. McDonald, E. M. Duffy, W. L. Jorgensen, *J. Am. Chem. Soc.* **1998**, *120*, 5104 – 5111.
[18] B. Dietrich, B. Dilworth, J.-M. Lehn, J.-P. Souchez, M. Cesario, J. Guilhem, C. Pascard, *Helv. Chim. Acta* **1996**, *79*, 569 – 587.
[19] B. Dietrich, J.-M. Lehn, J. Guilhem, C. Pascard, *Tetrahedron Lett.* **1989**, *30*, 4125 – 4129.
[20] S. D. Reilly, G. R. K. Khalsa, D. K. Ford, J. R. Brainard, B. P. Hay, P. H. Smith, *Inorg. Chem.* **1995**, *34*, 569 – 575.
[21] T. P. Straatsma, J. A. McCammon, *Annu. Rev. Phys. Chem.* **1992**, *43*, 407 – 435; P. Koolman, *Chem. Rev.* **1993**, *93*, 2395 – 2417.
[22] J. Cullinane, R. I. Gelb, T. N. Margulis, L. J. Zompa, *J. Am. Chem. Soc.* **1982**, *104*, 3048 – 3053.
[23] R. I. Gelb, B. T. Lee, L. J. Zompa, *J. Am. Chem. Soc.* **1985**, *107*, 909 – 916.
[24] D. A. Case, D. A. Pearlman, J. C. Caldwell, T. E. Cheatham III, W. S. Ross, C. L. Simmerling, T. A. Darden, K. M. Merz, R. V. Stanton, A. L. Cheng, J. J. Vincent, M. Crowley, D. M. Ferguson, R. J. Radmer, G. L. Seibel, U. C. Singh, P. K. Weiner, P. A. Kollman, *AMBER5*, University of California, San Francisco, **1997**.
[25] W. D. Cornell, P. Cieplak, C. I. Bayly, I. R. Gould, K. M. Merz, D. M. Ferguson, D. C. Spellmeyer, T. Fox, J. W. Caldwell, P. A. Kollman, *J. Am. Chem. Soc.* **1995**, *117*, 5179 – 5197.
[26] F. Berny, Ph.D. Thesis, Strasbourg, **2000**.
[27] W. L. Jorgensen, J. Chandrasekhar, J. D. Madura, *J. Chem. Phys.* **1983**, *79*, 926 – 936.
[28] P. E. Smith, W. F. van Gunsteren in *Computer Simulations of Biomolecular Systems* (Eds.: W. F. van Gunsteren, P. K. Weiner, A. J. Wilkinson), ESCOM, Leiden, **1993**, pp. 182 – 212.
[29] H. J. C. Berendsen, J. P. M. Postma, W. F. van Gunsteren, A. DiNola, *J. Chem. Phys.* **1984**, *81*, 3684 – 3690.
[30] I. G. Tironi, R. Sperb, P. E. Smith, W. F. van Gunsteren, *J. Chem. Phys.* **1995**, *102*, 5451 – 5459.
[31] E. Engler, G. Wipff in *Crystallography of Supramolecular Compounds* (Ed.: G. Tsoucaris), Kluwer, Dordrecht, **1996**, pp. 471 – 476.
[32] Y. Marcus, *Ion Solvation*, Wiley, Chichester, **1985**.

Received: May 22, 2000 [F2506]

  0947-6539/00/0623-4264 $ 17.50+.50/0 